



Universiteit  
Leiden  
The Netherlands

## **Radiology of colorectal cancer with emphasis on imaging of liver metastases**

Pijl, M.E.J.

### **Citation**

Pijl, M. E. J. (2005, January 25). *Radiology of colorectal cancer with emphasis on imaging of liver metastases*. Retrieved from <https://hdl.handle.net/1887/3487>

Version: Not Applicable (or Unknown)

License: [Licence agreement concerning inclusion of doctoral thesis in the Institutional Repository of the University of Leiden](#)

Downloaded from: <https://hdl.handle.net/1887/3487>

**Note:** To cite this publication please use the final published version (if applicable).



# 2

## Comparison of Inversion-Recovery Gradient- and Spin-Echo and Fast Spin-Echo Techniques in the Detection and Characterization of Liver Lesions

Milan E.J. Pijl, Martin N.J.M. Wasser, Els L. van Persijn van Meerten,  
Jan-Willem C. Gratama, Cornelis J.H. van de Velde, Jo Hermans,  
Aaldert Elevelt, Johan L. Bloem

*Radiology 1998; 209:427-434*

**ABSTRACT**

**Purpose:** To compare respiratory-triggered inversion-recovery (IR) gradient- and spin-echo (GRASE) magnetic resonance (MR) imaging with respiratory-triggered T2-weighted fast spin-echo (SE) imaging in the diagnosis of liver metastases.

**Materials and Methods:** In this prospective study, two radiologists independently identified focal hepatic lesions on respiratory-triggered IR GRASE and respiratory-triggered fast SE MR images in 28 consecutive patients with 186 (135 malignant and 51 benign) proved lesions. A combination of findings at surgery, intra-operative ultrasound, and histologic examination served as the standard of reference. Contrast-to-noise ratios (CNRs) were obtained from 86 lesions larger than 10 mm.

**Results:** The sensitivity in the detection of liver metastases was, independent of lesion size and observer, higher for IR GRASE imaging (55%) than for fast SE imaging (44%-50%) (observer 1,  $P = .014$ ; observer 2,  $P = .21$ ). Confidence levels with IR GRASE imaging were higher, but not significantly so, than those with fast SE imaging ( $P < .098$ ). Both observers characterized liver lesions better with IR GRASE than with fast SE imaging (observer 1,  $P = .04$ ; observer 2,  $P = .48$ ). The metastasis-liver CNR was significantly higher ( $P = .012$ ) with IR GRASE imaging.

**Conclusion:** The respiratory-triggered IR GRASE sequence is a fast alternative to the respiratory-triggered fast SE sequence in the evaluation of suspected liver metastases.

## INTRODUCTION

Fast spin-echo (SE) imaging, a technique based on rapid acquisition with relaxation enhancement (RARE) [1-4], in combination with either respiratory triggering [5,6] or breath holding [6,7], has enhanced the role of magnetic resonance (MR) imaging in the detection and characterization of focal hepatic lesions. Fast SE imaging has a more efficient method of k-space filling than does conventional SE imaging, thus enabling faster data acquisition. Each  $90^\circ$  pulse in fast SE imaging is followed by a train of  $180^\circ$  pulses, each producing a separate SE (Figure 1).

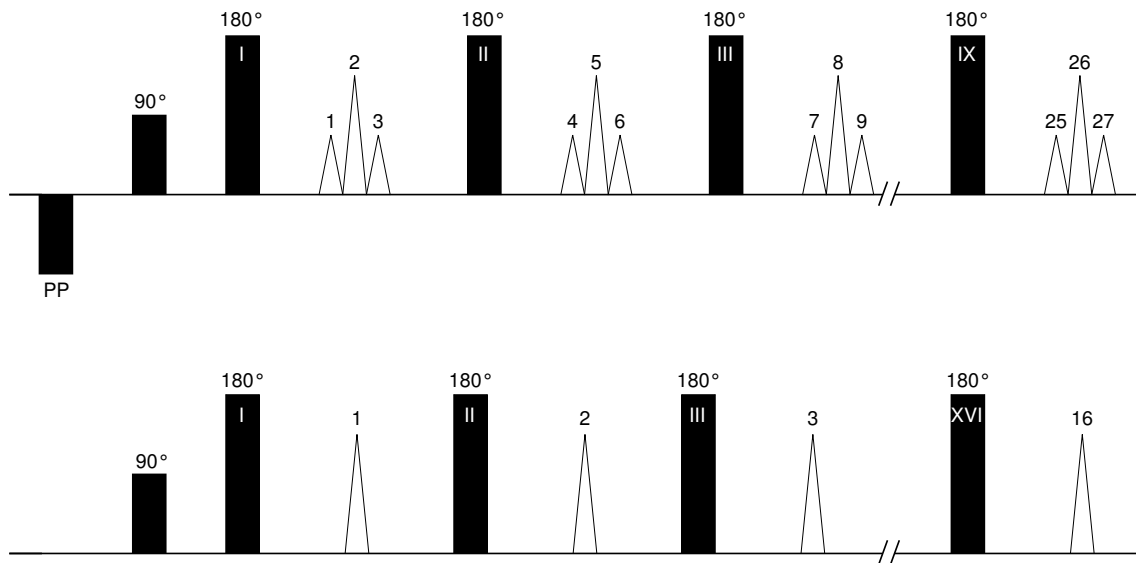


**Figure 1.** Diagrams display radio-frequency pulses (black bars) and received signal (open spikes) of the respiratory-triggered IR GRASE sequence (upper diagram) and respiratory-triggered fast SE sequence (lower diagram). The horizontal axis represents a time line with a length of one repetition time (equal for both sequences). Our fast SE sequence (ETL, 16) allows acquisition of 16 echoes in one repetition time. The GRASE sequence is a combination of fast SE and echo-planar imaging. Our IR GRASE sequence generates 27 echoes in one repetition time by generating three echoes (echo-planar imaging factor, 3) for each of the nine  $180^\circ$  refocusing pulses (ETL, 9). Arabic numbers above spikes represent the cumulative number of echoes. Roman numerals in black bars represent the cumulative number of  $180^\circ$  refocusing pulses. PP = pre-pulse.

A relatively new T2-weighted fast MR sequence is gradient- and spin-echo (GRASE) imaging [8]. The GRASE technique also consists of a  $90^\circ$  pulse followed by a train of  $180^\circ$  pulses but adds polarity switching of the readout gradients, which results in a train of radio-frequency-refocused SEs and a number of gradient-recalled echoes centered about each SE (Figure 1). More efficient use of the T2 decay period results in reduced acquisition time for both single- [9] and multishot GRASE imaging relative to RARE [10]. Additional advantages

of GRASE imaging over RARE are its lower deposition of radio-frequency power [8] and its higher signal-to-noise ratio [9].

The purpose of this study was to improve and accelerate multishot T2-weighted fast MR imaging of liver metastases. Therefore, the performance of multishot respiratory-triggered inversion-recovery (IR) GRASE imaging was prospectively evaluated in patients with liver metastases. On a lesion-by-lesion basis, the sensitivity and confidence levels in the detection of liver metastases, the ability to differentiate between malignant and benign focal hepatic lesions, and results of quantitative analysis of respiratory-triggered IR GRASE were compared with results of multishot respiratory-triggered fast SE imaging [1,5,6,11,12] and a standard of reference.

## **MATERIALS AND METHODS**

### **PATIENTS**

Between August 1995 and October 1996, 46 consecutive patients suspected or known to have liver metastases, referred to our hospital to undergo partial liver resection or isolated liver perfusion with melphalan (Alkeran<sup>®</sup>; Glaxo Wellcome, Zeist, The Netherlands) [13], were eligible for this prospective study. The study protocol was approved by the medical ethical committee of our hospital, and informed consent was obtained from all participating patients. The diagnosis at the time of referral was, in most cases, established by an increased serum level of tumor markers and findings at ultrasound (US).

In 15 patients, no standard of reference was available. Surgery was not performed in one patient because benign lesions, not metastases, were diagnosed during preoperative analysis. In two patients suspected extrahepatic tumor was confirmed at laparoscopy. In the 12 remaining patients, surgical therapy was not performed, either because it was no longer technically feasible or because of patient refusal. In three of the remaining 31 patients, more than 20 lesions appeared to be present. These three patients were excluded from this study because lesion-by-lesion correlation between MR sequences and the standard of reference was, in view of the tumor load, unrealistic.

Finally, 28 patients (19 men, nine women) aged 38-74 years (median age, 62 years) were included in this study. The primary malignancy was colorectal adenocarcinoma in 24 patients, leiomyosarcoma of the stomach in two patients, and follicular thyroid carcinoma in one

patient. In addition, one patient only had multiple hemangiomas, including one giant hemangioma necessitating surgery. The other 27 patients had at least one proved metastatic deposit. In none of the patients was relevant coexistent morbidity of the liver (e.g., cirrhosis or steatosis) diagnosed.

The median interval between preoperative MR examination and surgery was 25 days. With the exception of two patients, this interval was less than 10 weeks. In these two patients, in whom progressive disease was excluded by means of computed tomographic and intra-operative findings, treatment was delayed because of severe pulmonary problems.

#### MR IMAGING

The MR studies were performed with a 1.5-T system (Gyrosan NT 15; Philips Medical Systems, Best, The Netherlands) by using a quadrature body coil for signal transmission and reception. Respiratory triggering was used for both sequences, whereby repetition time was dependent on respiratory frequency. A belt around the upper abdomen generated respiratory triggering. During the examination, patients were not given special breathing commands. Image acquisition was started just before end expiration, allowing data acquisition during a period of reduced respiratory motion.

Both sequences were optimized for our MR system. The following parameters were identical for both sequences: transverse orientation, anterior-posterior phase-encoding direction, eighteen 10 mm thick sections with a 1 mm intersection gap, 375-400 mm field-of-view, 256 x 256 matrix, and four signals acquired per data line. The IR GRASE sequence had an effective echo time of 80 msec, echo spacing of 15 msec, inversion time of 150 msec (based on preliminary studies), echo train length (ETL) of nine, and echo-planar imaging factor (i.e., the number of gradient-recalled echoes) of three. The effective echo time, echo spacing and ETL for the fast SE sequence were 120 msec, 14 msec, and 16, respectively.

The average total imaging time, which was dependent on respiratory frequency, was 5 minutes for the IR GRASE sequence and 7 minutes for the fast SE sequence.

#### STANDARD OF REFERENCE

The standard of reference for all patients was based on the combination of findings at surgery, intra-operative ultrasound (IOUS), and histologic examination. After meticulous inspection of

the entire abdomen and complete mobilization of the liver, the surgeon palpated the liver bimanually. Then, IOUS was performed by two experienced radiologists (M.E.J.P., J.W.C.G.) in concert, having full knowledge of the pre-operative data. All liver segments were scanned with the US probe for preoperatively identified and questionable lesions and any additional lesions. A model 2000 system (Aloka, Tokyo, Japan) with a 7.5-MHz transducer tailored for IOUS procedures was used. The average duration of the IOUS investigation was 25 minutes. Examinations were recorded on videotape.

Histologic confirmation of at least one of the representative lesions was obtained in each patient. Using the defined standard of reference, we categorized lesions as either benign or malignant on the basis of histologic findings, consistency at palpation, characteristic appearance, and compressibility at IOUS. Lesions in the benign category were subsequently classified as cysts, hemangiomas, and miscellaneous lesions. Thus, we identified 186 focal hepatic lesions: 135 malignant and 51 benign (30 hemangiomas, 19 cysts, one granulomatous nodule, and one scar). The median number of lesions per patient was seven (range, 1-14). The localization of each lesion was categorized according to the Bismuth system [14].

The largest diameter of all lesions was assessed with IOUS; 95 lesions (61 malignant and 34 benign) were less than or equal to 10 mm and 91 (74 malignant and 17 benign) were larger than 10 mm. The median diameter of all lesions was 10 mm (range, 1.6-130 mm).

## DATA ANALYSIS

### *Qualitative Analysis*

Hard-copy images from all 28 patients were randomized and independently graded by two experienced MR radiologists (M.N.J.M.W., E.L.v.P.v.M.). Each reader separately evaluated one of the two MR sequences, blinded to all other test results, during several sessions. For the IR GRASE sequence, only the magnitude images were reviewed.

For each patient, the observers subjectively scored the overall image quality of the sequence by using a four-point scale: 1, good; 2, moderate; 3, suboptimal; 4, poor.

The observer noted the location, size, confidence level in diagnosis, and suspected nature of each lesion. The confidence level was scored by using a three-point scale: 1, definitely present; 2, probably present; 3, possibly present. The suspected nature of each lesion was graded with a five-point scale on the basis of signal intensity, morphology, and conspicuity,



where 1 was definitely benign and 5 was definitely malignant.

For the 186 lesions identified with the standard of reference, the presence, location, and suspected nature were compared to the findings of each observer and with each sequence. A lesion identified with the standard of reference but missed with an observer-sequence combination was classified as missed with that combination. Also, observers diagnosed both malignant and benign lesions that were not confirmed with the standard of reference. We labeled these false-positive lesions as artifacts or pseudolesions to avoid confusion with false-positive malignant lesions.

### *Quantitative Analysis*

Signal intensity was measured on a workstation with standard software and standard operator-defined regions of interest (ROIs). For the IR GRASE sequence, only the magnitude images were used.

Only lesions larger than 10 mm in diameter were analyzed because measurements of smaller lesions would not be sufficiently reliable owing to partial volume averaging. Four metastases could not be detected with MR imaging, even in retrospect. These metastases were, therefore, not included in this quantitative analysis. One scar lesion was also excluded from this analysis. Thus, quantitative analysis was performed in 86 lesions (70 malignant lesions, 11 hemangiomas and five cysts). The ROI within each lesion was placed in the largest possible homogeneous area available. In metastases with necrotic areas, the ROI was placed in the periphery of the lesion.

The ROI for hepatic parenchyma, spleen and background noise was an oval of 3 cm<sup>2</sup>. The ROI of the liver was located centrally in the right lobe, and the ROI of the spleen was also placed centrally. In liver and spleen, vessels were avoided as much as possible. Background noise was measured in the phase-encoding direction, ventral to the patient, at the level of the right liver lobe, to include both systematic and motion-related noise [11,15].

The lesion-liver contrast-to-noise ratio (CNR) was calculated as the difference between the signal intensities of lesion and liver divided by the standard deviation of background noise [15].

## STATISTICAL ANALYSIS

The Wilcoxon signed-rank test was used to compare the subjective overall image quality with both sequences, and the two-tailed Student *t* test was used to compare the mean scores for overall image quality.

Statistical analysis of qualitative data for small ( $\leq 10$  mm) and large ( $> 10$  mm) lesions was performed separately if the number of lesions per size category was sufficient. If the number of lesions in any size category was insufficient to allow separate statistical analysis, the analysis was performed with cumulative data. For sensitivity calculations and interobserver variability analysis, a lesion detected on MR images was considered malignant if an observer rated it definitely malignant (score of 5) or probably malignant (score of 4).

The sensitivities of the IR GRASE and fast SE sequences were compared by using the McNemar test. The Wilcoxon signed-rank test was used to compare the confidence levels with both sequences.

The study of interobserver variability was restricted to liver metastases proved with the standard of reference and was analyzed by means of  $\kappa$  statistics. The  $\kappa$  values greater than zero were considered to indicate positive correlation, values of 0.00-0.40 were considered to indicate poor correlation, values of 0.41-0.75 were considered to indicate good correlation, and values greater than 0.75 were considered to indicate excellent correlation.

Receiver operated characteristic (ROC) analysis was performed on the characterization of lesions. Artifacts and missed lesions were excluded from this analysis because the dichotomous character of the ROC analysis would be hampered. ROC curves were used to compare sequences. The ROC curves were fitted with the use of the maximum likelihood method as implemented in the ROCFIT program (Metz CE, University of Chicago, Ill.). Second, with use of the CORROC2 program (Metz CE, University of Chicago, Ill.), areas under the ROC curves were calculated and evaluated for significant differences between the sequences. In this second analysis, only lesions detected with both sequences by each observer were taken into account, as the CORROC2 program is designed for paired data.

Statistical analysis of the lesion-liver CNR per sequence was done by using the one-way analysis of variance, with the least-significant difference multiple comparison test for post hoc testing. The lesion-liver CNR per lesion type was compared by using the two-tailed Student *t* test.

For all tests used, a *P* value of less than .05 was considered statistically significant.

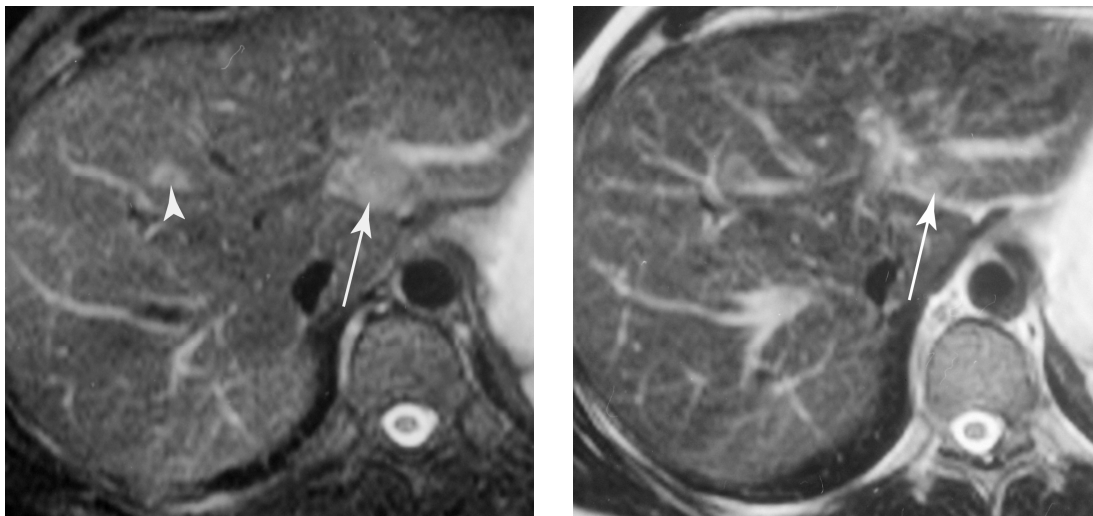
## RESULTS

### IMAGE QUALITY

On a four-point scale, the mean subjective overall image quality scores for the fast SE and IR GRASE sequences were, respectively,  $1.46 \pm 0.84$  and  $1.75 \pm 1.0$  ( $P = .15$ ) for observer 1 and  $1.29 \pm 0.46$  and  $1.79 \pm 0.83$  ( $P = .002$ ) for observer 2.

The subjective image quality of fast SE images was judged to be better than that of IR GRASE images in 11 and 13 patients by observers 1 ( $P = .17$ ) and 2 ( $P = .005$ ), respectively. Similar ratings for overall image quality were noted in 13 patients by both observers.

Both observers considered the signal void of through-plane intra-hepatic vessels displayed on IR GRASE images advantageous over the high signal intensity vessels seen on fast SE images (Figure 2), especially with regard to lesion detection.



**a.**

**b.**

**Figure 2.** (a) IR GRASE image clearly demonstrates a small liver metastasis (arrowhead) adjacent to hepatic veins. The signal void in the intrahepatic vessels facilitates detection of liver metastasis. (b) On the fast SE image, the metastasis is less conspicuous. Note the partial volume of the metastasis in segment II (arrow) on both images.

### LESION DETECTION

The sensitivity of both sequences for depicting metastases was markedly influenced by the size of the lesion (Table 1). Both observers detected more lesions, independent of size, with the IR GRASE sequence than with the fast SE sequence (Figure 3). These differences were statistically significant only for observer 1 ( $P = .014$ ).

**Table 1.** Sensitivity for the Detection of Metastases According to Lesion Size.

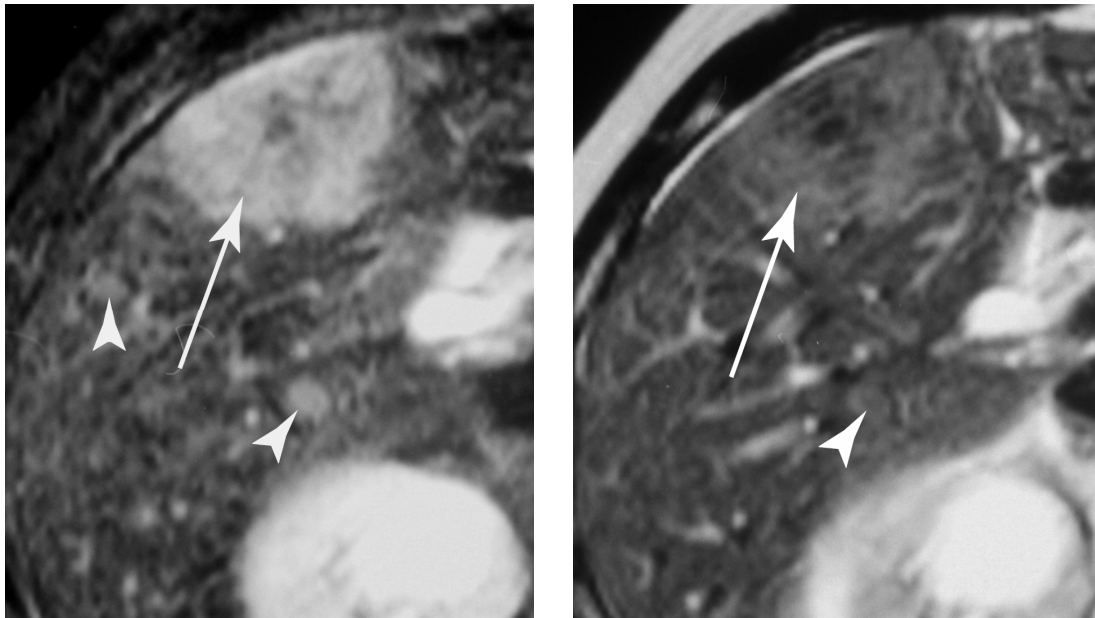
Parameter	Lesions $\leq$ 10 mm (n=61)		Lesions $>$ 10 mm (n=74)		All Metastases (n=135)	
	Obs. 1	Obs. 2	Obs. 1	Obs. 2	Obs.1	Obs. 2
No. of metastases detected with IR GRASE	11 (18)	10 (16)	63 (85) <sup>#</sup>	64 (86)	74 (55) <sup>†</sup>	74 (55)
No. of metastases detected with fast SE	6 (10)	7 (11)	54 (73) <sup>#</sup>	60 (81)	60 (44) <sup>†</sup>	67 (50)
No. of metastases detected with both sequences	2 (3)	3 (5)	51 (69)	56 (76)	53 (39)	59 (44)
No. of metastases missed with both sequences	46 (75)	47 (77)	8 (11)	6 (8)	54 (40)	53 (39)

The difference in metastases detection between the two sequences was statistically significant only for observer 1 for <sup>#</sup>lesions measuring more than 10 mm ( $P = .035$ ) and <sup>†</sup>all lesions ( $P = .014$ ). Numbers in parentheses are percentages. Obs. = observer.

Confidence levels for the detection of liver metastases were marginally better with IR GRASE imaging than with fast SE imaging (Figure 4). The mean confidence level of observer 1 ( $n = 53$ ) in the detection of malignant lesions, irrespective of size, was  $1.00 \pm 0.00$  for IR GRASE imaging and  $1.13 \pm 0.48$  for fast SE imaging ( $P = .098$ ). The mean confidence level of observer 2 in the detection of malignant lesions ( $n = 59$ ) was  $1.07 \pm 0.31$  for IR GRASE imaging and  $1.17 \pm 0.53$  for fast SE imaging ( $P = .084$ ).

The observers scored a total of 62 artifacts or pseudolesions that could not be confirmed with the standard of reference. On MR images, 36 artifacts or pseudolesions were 10 mm or smaller and 26 were larger than 10 mm. Observer 1 found 25 artifacts with the IR GRASE sequence and 20 with the fast SE. Fifteen of the 25 artifacts were diagnosed as malignant lesions with both sequences. Observer 2 found 16 artifacts with IR GRASE imaging and 17 with fast SE imaging, of which 13 and 14, respectively, were diagnosed as malignant lesions.

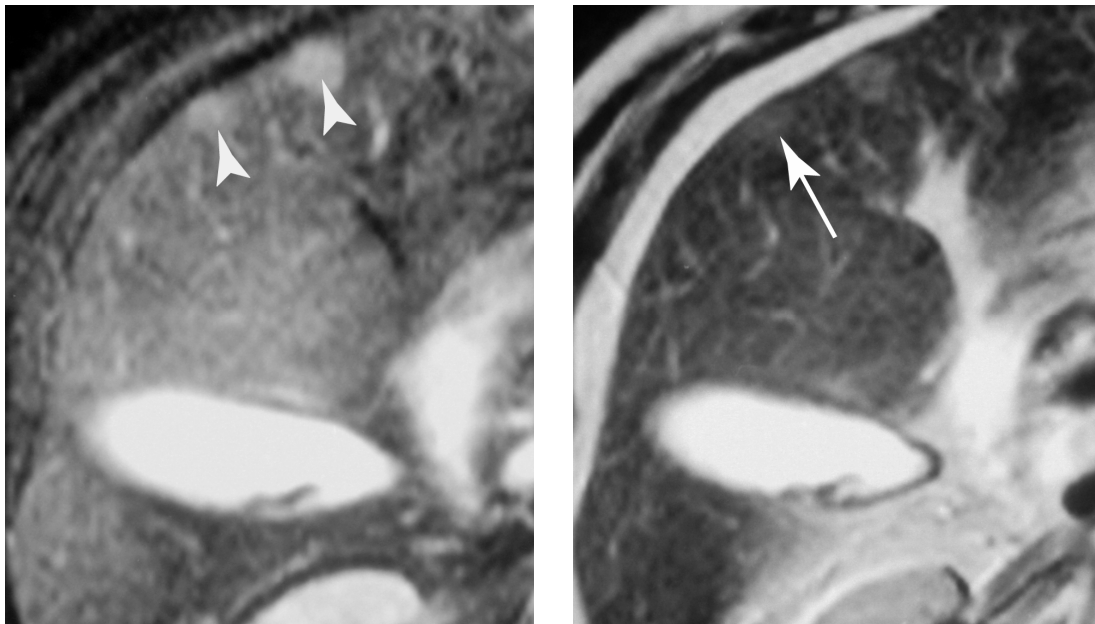
Observer 1 identified one artifact with both sequences; observer 2 identified four artifacts with both sequences (Figure 5).



a.

b.

**Figure 3.** Images demonstrate the superior sensitivity of the IR GRASE sequence in the detection of liver metastases. (a) IR GRASE image shows a large metastasis (arrow) in segment IV-B and two small metastases (arrowheads) in segment V. (b) Fast SE image shows the large metastasis (arrow). One of the small metastases (arrowhead) was found at retrospective analysis of the image. The second small metastasis is not seen.



a.

b.

**Figure 4.** Images demonstrate the better confidence levels for metastases detection with the IR GRASE sequence. (a) IR GRASE image clearly demonstrates two small metastases (arrowheads). (b) Fast SE image also demonstrates both metastases, but the confidence level is lower, especially for the most lateral metastasis (arrow).

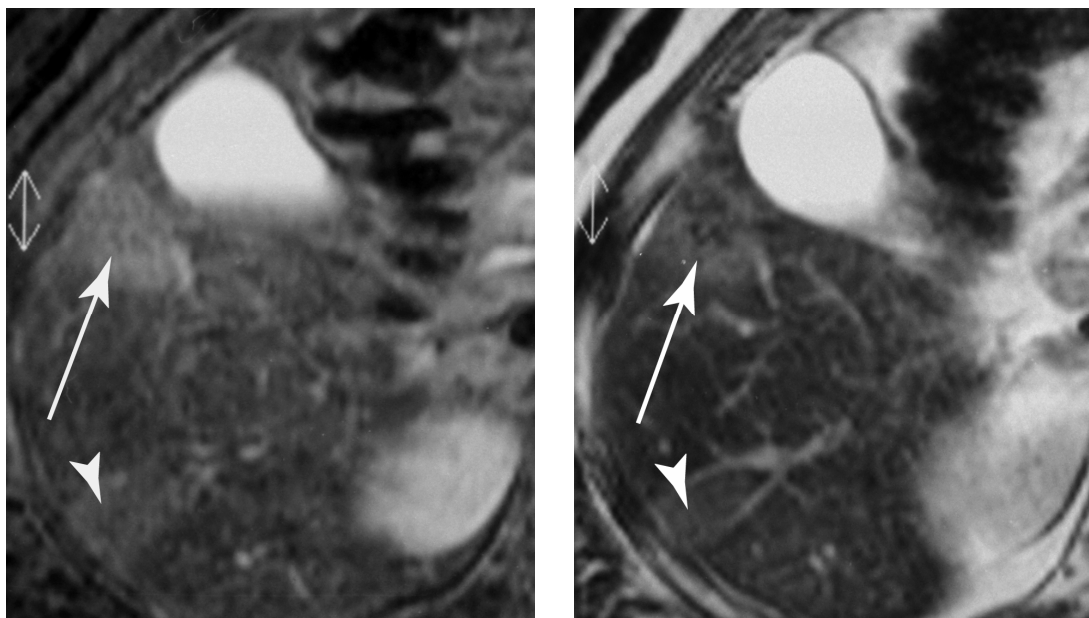


**Figure 5.** Pseudolesion. (a) IR GRASE and (b) fast SE images show a metastasis (arrow), which was confirmed with the standard of reference, in segment V. Observer 2 diagnosed a second metastasis (arrowhead) in segment VI, but it could not be confirmed with the standard of reference (no focal lesion was found).

#### INTEROBSERVER VARIABILITY

The  $\kappa$  values for detecting liver metastases were higher for the IR GRASE sequence than for the fast SE (Table 2). The largest difference in  $\kappa$  values was noted for the large lesions, where observer agreement was excellent for IR GRASE imaging ( $\kappa = 0.80$ ) and good for fast SE ( $\kappa = 0.61$ ). Observer agreement was largest ( $\kappa = 0.82$ ) for the IR GRASE sequence and both size categories combined.

**Table 2.** Interobserver Variability for the Detection of Liver Metastases.

Lesion size	No. of Liver Metastases	$\kappa$ Value <sup>#</sup> IR GRASE	$\kappa$ Value <sup>#</sup> Fast SE
All metastases	135	$0.82 \pm 0.05$	$0.78 \pm 0.05$
> 10 mm	74	$0.80 \pm 0.13$	$0.61 \pm 0.17$
$\leq 10$ mm	61	$0.55 \pm 0.11$	$0.52 \pm 0.12$

<sup>#</sup> Data are the mean  $\pm$  standard error of the mean.

## CHARACTERIZATION

ROC analysis of the accuracy with which focal hepatic lesions were characterized, irrespective of size, revealed that IR GRASE imaging was superior to fast SE imaging (Figures 6, 7).

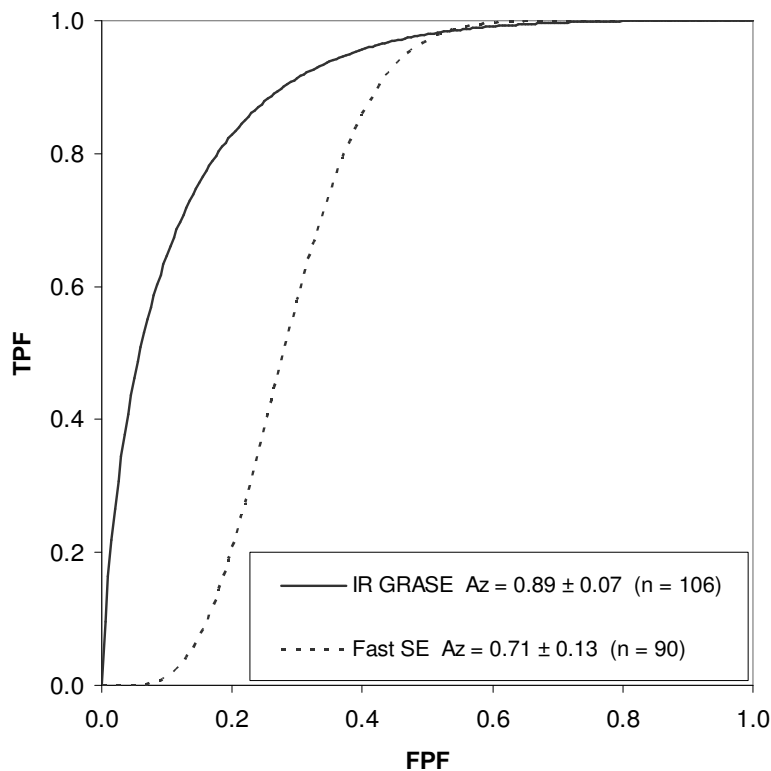


**Figure 6.** ROC curves indicate the accuracies with which focal hepatic lesions were characterized with both sequences by observer 1.

*FPF* = false-positive fraction, *TPF* = true-positive fraction.

Pair-wise comparison for observer 1 ( $n = 81$ ) gave areas under the ROC curve ( $A_z$ ) of  $0.97 \pm 0.04$  for IR GRASE imaging and  $0.74 \pm 0.13$  for fast SE imaging ( $P = .04$ ). Observer 2 ( $n = 83$ ) had  $A_z$  values of  $0.99 \pm 0.01$  for IR GRASE imaging and  $0.99 \pm 0.02$  for fast SE imaging ( $P = .48$ ).

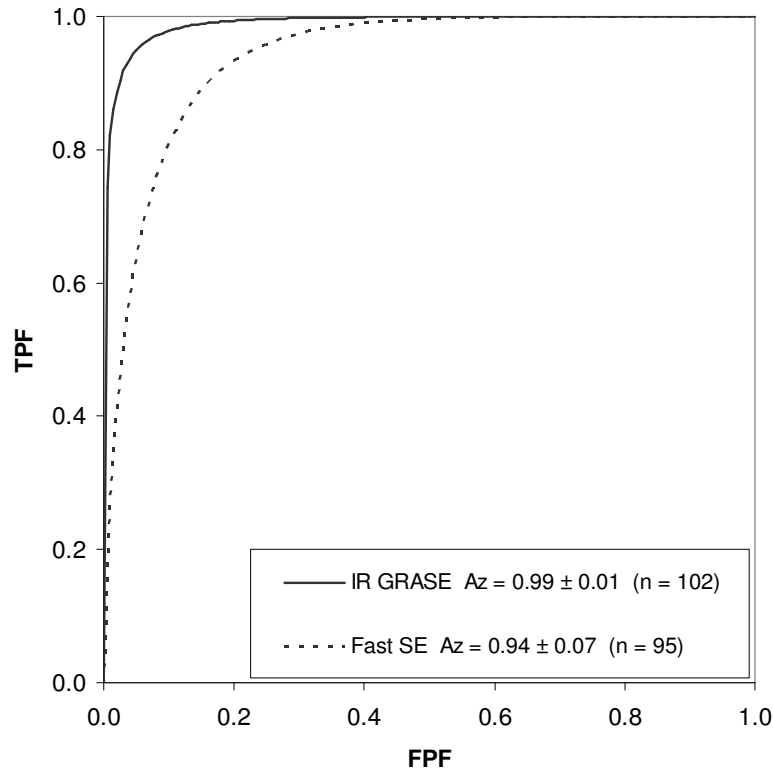


**Figure 7.** ROC curves indicate the accuracies with which focal hepatic lesions were characterized with both sequences by observer 2.

*FPF* = false-positive fraction, *TPF* = true-positive fraction.

### CNRs

The lesion-liver CNR for both sequences differed significantly among malignant lesions, hemangiomas, and cysts (Table 3, Figure 8). The metastasis-liver CNR was significantly higher with the IR GRASE sequence than with the fast SE sequence ( $P = .012$ ).

**Table 3.** Results of Quantitative Analysis.

Lesion Type	No. of Lesions	CNR at IR GRASE <sup>#</sup>	CNR at Fast SE <sup>#</sup>	<i>P</i> Value <sup>†</sup>
Malignant	70	19.1 ± 18.2	16.5 ± 21.7	.012
Hemangioma	11	49.0 ± 20.3	39.6 ± 15.6	.15
Cyst	5	57.6 ± 38.6	64.3 ± 32.1	.35

For both sequences, the CNR of malignancies differs significantly from those of hemangiomas and cysts ( $P \leq .002$ ). For fast SE imaging, the CNR of hemangiomas differs significantly from that of cysts ( $P = .038$ ).

<sup>#</sup> Data are mean lesion-liver CNR ± SD.

<sup>†</sup> Determined with the Student *t* test.



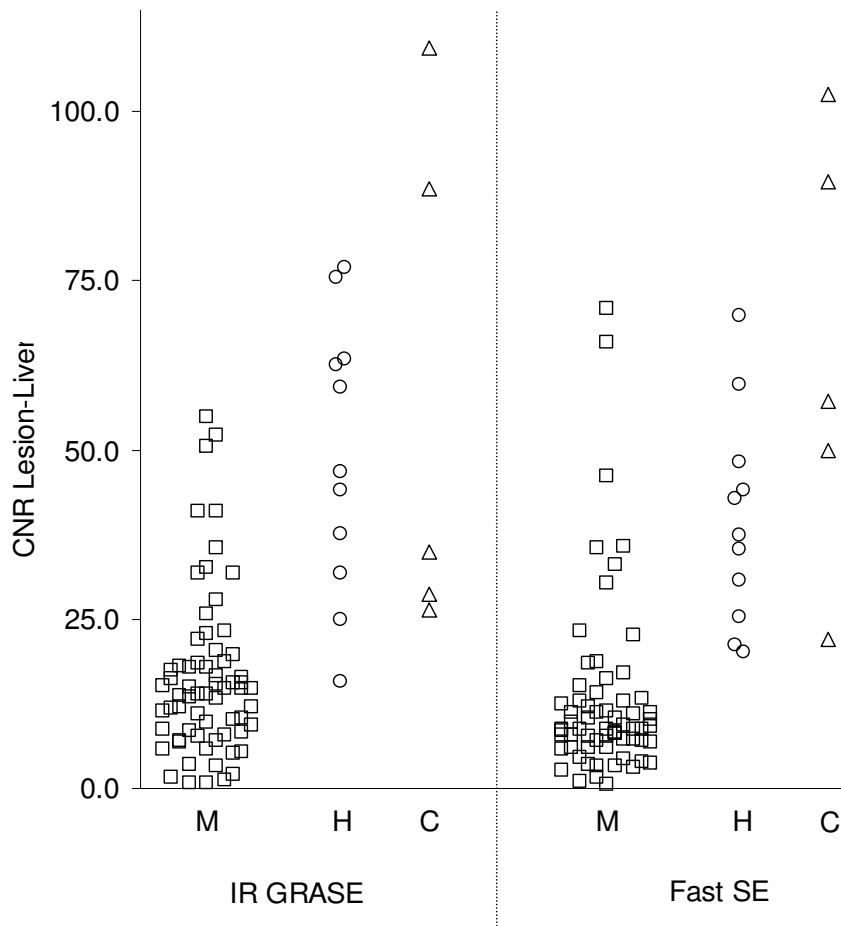


**Figure 8.** Results of quantitative analysis. Scatterplot shows lesion-liver CNR for both sequences. C = cyst, H = hemangioma, M = malignancy.

## DISCUSSION

In the continuing search for the optimal MR pulse sequence to use in the detection of liver metastases, the respiratory-triggered IR GRASE sequence appears to be a new competitor. In this prospective study, the sensitivity of respiratory-triggered IR GRASE sequence in the detection of liver metastases was found to be superior to that of the respiratory-triggered fast SE sequence. Apart from the superior sensitivity for liver metastases, the confidence level of both observers for detection was also higher with respiratory-triggered IR GRASE imaging than with respiratory-triggered fast SE imaging. Furthermore, observer agreement for the detection of liver metastases and differentiation of malignant from benign focal hepatic lesions was better with the IR GRASE sequence.

The subjective quality of the IR GRASE images was, in accordance with findings of Jung

et al [10] but contrary to the results of Feinberg et al [8,9], inferior to that of fast SE images. Despite the use of respiratory triggering, the IR GRASE sequence was more susceptible to image blur, especially in patients with irregular breathing. Both observers appreciated the signal void of through-plane intrahepatic vessels on the IR GRASE images. The higher sensitivity of gradient sequences for susceptibility effects and turbulent flow might explain this signal void. In-plane vessels, which are readily recognizable as vascular structures, do not display this signal void owing to in-plane saturation. This feature could be beneficial in the detection of small metastases, especially those adjacent to vessels. Detection of small liver metastases was better with IR GRASE imaging than with fast SE imaging (Figure 3, Table 1), although the difference was not statistically significant.

The sensitivity in the detection of liver metastases decreased with decreased lesion diameter (Table 1). Decreasing the section thickness to, for instance, 8 mm could have increased sensitivity somewhat, but, in accordance with previous studies [16-18], detection of lesions smaller than 10 mm was insufficient with both the fast SE and IR GRASE sequences. In our study, the overall sensitivity in the detection of liver metastases (large and small lesions) was low because 45% of the malignant lesions were 10 mm or less in diameter, a percentage not previously published in the MR imaging literature. When lesion size is taken into account, our results fit in the ranges given in previously published articles [16,17]. Hagspiel et al [16] detected none of the six metastases smaller than 5 mm and only up to four of 11 metastases smaller than 10 mm with various MR imaging techniques.

Because benign hepatic lesions are often visualized incidentally, it is necessary to differentiate them from malignant lesions. In this study, the IR GRASE sequence was, irrespective of lesion size and observer, superior to the fast SE sequence in the differentiation of malignant from benign focal hepatic lesions, as was shown by larger areas under the ROC curve and smaller standard deviations (Figures 6, 7). In the pair-wise comparison, this positive trend reached statistical significance only for observer 1 ( $P = .04$ ).

Similar to previous studies for single- [8,9] and multishot [10] GRASE imaging, the metastases-liver CNR was significantly higher for the multishot IR GRASE sequence than for the fast SE sequence ( $P = .012$ ). We consider this an important advantage of respiratory-triggered IR GRASE sequence because lesion detection depends largely on lesion-liver CNR; this may well explain its superior performance.

In the quantitative analysis of both sequences, benign and malignant lesions could be well differentiated.

There are some limitations to this study. First, both sequences were optimized in pilot studies for our system with body coils and respiratory triggering. The ETL of 16 used with the fast SE sequence may decrease lesion-liver CNR and, therefore, detection of small lesions. Conversely, half-Fourier single-shot turbo SE imaging successfully uses an even longer ETL, up to 120 [4,6]. Although the use of an echo time shorter than 120ms might increase sensitivity, it will decrease characterization, which is also an important element of liver imaging. Second, because only the magnitude images of the IR GRASE sequence were reviewed, we did not use the entire range of contrast of real images. In this study, though, the metastases-liver CNR for the IR GRASE magnitude images was already superior to that of fast SE images. Third, high pretest probability (known primary malignancy and liver metastases) in these selected patients could well incite the observer to overread, resulting in a relatively high number of artifacts or pseudolesions that were thought to be malignant. Furthermore, in daily practice, this number of (malignant) pseudolesions will probably be lower because the MR examination is not read sequence by sequence, but as a whole. Finally, respiratory-triggered IR GRASE imaging was not compared with fat-suppressed respiratory-triggered fast SE imaging, but with a previously evaluated non-fat-suppressed fast SE sequence [1,5,6,11,12]. It has been shown, however, that the added value of fat suppression in the detection of focal hepatic lesions with a hybrid RARE is limited [19]. Furthermore, adding fat suppression to the respiratory-triggered fast SE sequence would even further increase imaging time, and one of our goals was to accelerate T2-weighted MR imaging.

Although the detection of small liver metastases remains a problem, the respiratory-triggered IR GRASE sequence may be useful for detecting and characterizing focal hepatic lesions because it has a higher metastasis-liver CNR ( $P = .012$ ) and a shorter imaging time than does the respiratory-triggered fast SE sequence. Both observers detected more metastases with higher confidence levels with the IR GRASE sequence than with the fast SE sequence, although this difference was significant with only one observer. Characterization of liver lesions was also improved (statistically significant in one observer) with respiratory-triggered IR GRASE imaging.

## REFERENCES

1. Schwartz LH, Seltzer SE, Tempny CM, et al. Prospective comparison of T2-weighted fast spin-echo, with and without fat suppression, and conventional spin-echo pulse sequences in the upper abdomen. *Radiology* 1993; 189:411-416.
2. Mitchell DG, Outwater EK, Vinitzki S. Hybrid RARE: implementations for abdominal MR imaging. *J Magn Reson Imaging* 1994; 4:109-117.
3. Catasca JV, Mirowitz SA. T2-weighted MR imaging of the abdomen: fast spin-echo vs conventional spin-echo sequences. *AJR* 1994; 162:61-67.
4. van Hoe L, Bosmans H, Aerts P, et al. Focal liver lesions: fast T2-weighted MR imaging with half-Fourier rapid acquisition with relaxation enhancement. *Radiology* 1996; 201:817-823.
5. Low RN, Alzate GD, Shimakawa A. Motion suppression in MR imaging of the liver: comparison of respiratory-triggered and nontriggered fast spin-echo sequences. *AJR* 1997; 168:225-231.
6. Tang Y, Yamashita Y, Namimoto T, Abe Y, Takahashi M. Liver T2-weighted MR imaging: comparison of fast and conventional half-Fourier single-shot turbo spin-echo, breath-hold turbo spin-echo, and respiratory-triggered turbo spin-echo sequences. *Radiology* 1997; 203:766-772.
7. Rydberg JN, Lomas DJ, Coakley KJ, Hough DM, Ehman RL, Riederer SJ. Comparison of breath-hold fast spin-echo and conventional spin-echo pulse sequences for T2-weighted MR imaging of liver lesions. *Radiology* 1995; 194:431-437.
8. Feinberg DA, Kiefer B, Johnson G. GRASE improves spatial resolution in single shot imaging. *Magn Reson Med* 1995; 33:529-533.
9. Feinberg DA, Oshio K. GRASE (gradient- and spin-echo) MR imaging: a new fast clinical imaging technique. *Radiology* 1991; 181:597-602.
10. Jung G, Krahe T, Kugel H, et al. Prospective comparison of fast SE and GRASE sequences and echo planar imaging with conventional SE sequences in the detection of focal liver lesions at 1.0 T. *J Comput Assist Tomogr* 1997; 21:341-347.
11. Siewert B, Muller MF, Foley M, Wielopolski PA, Finn JP. Fast MR imaging of the liver: quantitative comparison of techniques. *Radiology* 1994; 193:37-42.
12. Outwater EK, Mitchell DG, Vinitzki S. Abdominal MR imaging: evaluation of a fast spin-echo sequence. *Radiology* 1994; 190:425-429.
13. Vahrmeijer AL, van Dierendonck JH, van de Velde CJH. Treatment of colorectal cancer metastases confined to the liver. *Eur J Cancer* 1995; 31A:1238-1242.
14. Bismuth H. Surgical anatomy and anatomical surgery of the liver. *World J Surg* 1982; 6:3-9.

15. Hendrick RE. Measurement of signal, noise, and SNR in MR Images. In: Hendrick RE, Russ PD, Simon JH, eds. MRI: principles and artifacts. 1st ed. New York: Raven Press Ltd., 1993; 2-6.
16. Hagspiel KD, Neidl KF, Eichenberger AC, Weder W, Marincek B. Detection of liver metastases: comparison of superparamagnetic iron oxide-enhanced and unenhanced MR imaging at 1.5 T with dynamic CT, intraoperative US, and percutaneous US. *Radiology* 1995; 196:471-478.
17. Hamm B, Mahfouz AE, Taupitz M, et al. Liver metastases: improved detection with dynamic gadolinium-enhanced MR imaging? *Radiology* 1997; 202:677-682.
18. Oudkerk M, van den Heuvel AG, Wielopolski PA, Schmitz PI, Borel Rinkes IHM, Wiggers TW. Hepatic lesions: detection with ferumoxide-enhanced T1-weighted MR imaging. *Radiology* 1997; 203:449-456.
19. Soyer P, de Givry SC, Gueye C, Lenormand S, Somveille E, Scherrer A. Detection of focal hepatic lesions with MR imaging: prospective comparison of T2-weighted fast spin-echo with and without fat suppression, T2-weighted breath-hold fast spin-echo, and gadolinium chelate-enhanced 3D gradient-recalled imaging. *AJR* 1996; 166:1115-1121.